Determination of the Rashba and Dresselhaus Spin–Orbit Interaction Parameters and g-Factor from the Critical Points of the Spectrum in a 2D Electron Gas in an In-Plane Magnetic Field

Yurii Ya Tkach

A 2D electron gas with spin–orbit interaction (SOI) is known to form an anisotropic system with van Hove singularities controllable by a parallel magnetic field. The conductivity tensors of this system in the presence of both Rashba and Dresselhaus SOIs is studied. It is found that the diagonal elements of the conductivity tensor have sharp dips when the Fermi level passes through the singularity point of a spectrum. The energy position of these dips at different orientations of the magnetic field allows one to determine both SOI constants and the Landé g-factor. The dependencies of the surface charge concentration on the Fermi level show a sharp change in the slope near the minimum of the spectrum due to the jumps of the density of states, while the van Hove singularities are not noticeable. In a zero magnetic field, the conductivity tensor has off-diagonal terms which change the sign when the Fermi level passes the saddle points of the spectrum. The off-diagonal terms evidence the appearance of the Hall voltage caused by the anisotropy of the Fermi surface and the scattering process.

1. Introduction

Spin effects in a 2D electron gas (2DEG) are the subject of intensive studies to search new principles for the operation of spintronic devices.[1,2] To manipulate the spin by an electric field, the Rashba[3] and Dresselhaus[4] spin–orbit interaction (SOI) are used, which are often present together in many systems.

A study of the SOI parameters is mainly based on measurements of magnetotransport phenomena: Shubnikov–de Haas oscillations, the anisotropic spin photocurrent, the anisotropy of the Raman effect, the weak antilocalization, the anisotropic spin relaxation by the Hanle effect, and the Kerr and Faraday effects. Interesting methods for studying the parameters of SOI, based on the geometric focusing of the electron beam by a transverse magnetic field in the presence of in-plane magnetic

Dr. Y. Y. Tkach
Kotel'nikov Institute of Radio Engineering and Electronics
Russian Academy of Sciences
Moscow District, Fryazino 141190, Russia
E-mail: tkach@ms.ire.rssi.ru

The ORCID identification number(s) for the author(s) of this article can be found under https://doi.org/10.1002/pssb.202000553.

field were considered recently.[5,6] These techniques are described in more detail in the reviews.[7–10]

Determining the SOI parameters is not an easy task, often requiring in addition to precision measurements, the special geometry of the samples.[11] Many methods give only the ratio between the Rashba and Dresselhaus constants or allow one to determine only one type of spin splitting, so useful techniques are needed to define the SOI parameters.

Recently, we showed[12] that applying a parallel magnetic field to 2DEG with SOI results in sharp peaks of a density of states controllable by this field due to saddle points of the energy dispersion (van Hove singularity).[13] Such sharp features must manifest themselves in transport properties. One of the main problems in the study of anisotropic transport is that in this case the relaxation time approximation cannot be used to solve the Boltzmann kinetic equation.[14–16] A method allowing to solve this problem in the semiclassical approximation for low temperatures and elastic scattering of electrons by impurities with a short-range potential was developed in the article.[17] The point is that the integral kinetic equation is the Fredholm integral equation with a degenerate kernel. Therefore, it reduces to an algebraic one and can be exactly solved. It was shown[17,18] that in 2DEG with the Rashba SOI and an in-plane magnetic field, the van Hove singularities lead to sharp dips in the longitudinal conductivity and spin polarization induced by a charge current (Aronov–Landa–Geller–Edelstein effect;[19,20] see a modern interpretation of this effect in ref. [21]).

The interplay of the SOI and a parallel magnetic field in 2DEG is of considerable interest, because the magnetic field allows one to manipulate the Fermi contours in a controllable manner, which is an effective tool for studying electronic states and scattering processes. When the magnetic field is oriented at an arbitrary angle with respect to the plane of the 2DEG, the spectrum and orbital motion of the electrons undergoes a substantial change.[22] That is why the in-plane magnetic field is attractive, because a change in its intensity does not disturb the orbital wave functions, but changes the Fermi contours. This allows one to study the influence of the Fermi-contour topology on the electron transport.

In this work, we expand the scope of the previous work by including both the Rashba and Dresselhaus-type SOIs. We examine a 2D gas of noninteracting electrons with the Rashba and Dresselhaus SOIs in the presence of a parallel magnetic field. The magnetic field leads to the appearance of the van Hove singularities[12] in the density of states, which strongly affect the transport properties and enhance the anisotropy of the Fermi contours. We calculate the conductivity tensor and study how it changes with increasing magnetic field at a given Fermi level or changing the Fermi level at a constant magnetic field. It was found that the diagonal components of the conductivity tensor have sharp dips occurring when the Fermi energy passes through the van Hove singularities. Moreover, the direction of the highest conductivity changes near this energy. The presence of two SOIs leads to the anisotropy of the Fermi surface and the anisotropy of scattering even in a zero magnetic field. This leads to the nonzero off-diagonal terms of the conductivity tensor, which indicates the appearance of a Hall voltage without a magnetic field. The inclusion of a magnetic field enhances this effect. Using the results of the article,[23] in which the dispersion of 2DEG with Rashba and Dresselhaus SOIs in a parallel magnetic field was studied in detail, we show how to determine the SOI parameters and the Landé factor from measurements of the dependencies of the conductivity on the magnetic field or the position of the Fermi level near van Hove singularities for different orientations of the magnetic field.

We have not considered the Coulomb interaction, although at present it also attract a lot of attention of researchers.[24,25] This is justified when the SOI energy E_{so} is higher than the Coulomb energy of the electron–electron interaction E_{ee}. Materials and structures with a large E_{so} of the order of 0.1 eV are found and been actively investigated now. It is enough to mention BiTeI, the LaAlO$_3$/SrTiO$_3$ interface, and surface alloys. For example BiTeI with energy $E_{so} = 0.1$ eV, at the maximal concentration at which only the lower spin subband is filled $n_0 = 1.9 \times 10^{13}$ cm^{-2}, the Coulomb energy $E_{ee}(n_0) = 0.04$ eV.[26,27]

2. Hamiltonian and Electronic States

In this section, we give the Hamiltonian and wave functions that are used to calculate transport properties. The spectrum of 2D electrons with the Rashba and Dreselhause SOIs in an in-plane magnetic field was considered in ref. [12,28]. In more detail, the spectrum was studied in a recent article.[23]

The Hamiltonian has the following form

$$H = \frac{\mathbf{p}^2}{2m}\sigma_0 + \frac{\alpha}{\hbar}(p_x\sigma_y - p_y\sigma_x) + \frac{\beta}{\hbar}(p_x\sigma_x - p_y\sigma_y) - \frac{g^*}{2}\mu_B\mathbf{B}\sigma \quad (1)$$

where $\mathbf{p} = (p_x, p_y)$ is the electron momentum, m is the effective mass, α and β are the constants of Rashba and Dresselhouse SOIs, σ_x and σ_y are Pauli matrices, $\mathbf{B} = B(\cos\zeta, \sin\zeta, 0)$ is a magnetic field strength, μ_B is the Bohr magneton. g^* is the effective Landé factor, which is assumed to be isotropic and independent of B. The vector potential A is written in the gauge $\mathbf{A} = (0, 0, \gamma B\cos\zeta - xB\sin\zeta)$.

There are two types of eigenstates, which we will mark by the index $\lambda = \pm$. Their energies and wave functions have the form

$$\varepsilon_\lambda(\mathbf{k}) = k^2 + 2\lambda g(\mathbf{k}, \mathbf{b}, \gamma) \quad (2)$$

and

$$\psi_{\mathbf{k}\lambda}(\mathbf{r}) = \frac{1}{\sqrt{2S^*}}\begin{pmatrix} 1 \\ i\lambda e^{i\varphi} \end{pmatrix} e^{i(k_x x + k_y y)} \quad (3)$$

Here and in the following we use dimensionless quantities: ε is the energy normalized to the characteristic SOI energy $E_{so} = m\alpha^2/(2\hbar^2)$; $\mathbf{k}$ is the wave vector normalized to $k_{so} = \alpha m/\hbar^2$; $\mathbf{b} = g\mu_B\mathbf{B}\hbar^2/(2m\alpha^2)$ — dimensionless magnetic field, $g(\mathbf{k}, \mathbf{b}, \gamma) = \sqrt{(k_x - \gamma k_y - b_y)^2 + (k_y - \gamma k_x + b_x)^2}$, $\gamma = \beta/\alpha$, S^* is a normalization area.

The phase $\varphi(\mathbf{k})$ is determined by the relations

$$\sin\varphi = \frac{(k_y - \gamma k_x + b_x)}{g(\mathbf{k}, \mathbf{b}, \gamma)} \quad (4)$$

$$\cos\varphi = \frac{(k_x - \gamma k_y - b_y)}{g(\mathbf{k}, \mathbf{b}, \gamma)} \quad (5)$$

Without a magnetic field, the energy landscape in $\mathbf{k}$-space is centrosymmetric $\varepsilon_\lambda(\mathbf{k}) = \varepsilon_\lambda(-\mathbf{k})$ and has two symmetry axes: $k_x = \pm k_y$. In the lower spin subband, there are two minimums, ε_-^m, with the same energy $\varepsilon_-^m = -(1 + \gamma)^2$ in different points $\pm((1 + \gamma)/\sqrt{2}, (1 + \gamma)/\sqrt{2})$ of the $\mathbf{k}$-space, as well as two saddle points, ε_-^s, with energy $\varepsilon_{-s} = -(1 - \gamma)^2$ and coordinates $(\pm(1 - \gamma)/\sqrt{2}, \mp(1 - \gamma)/\sqrt{2})$ in the $\mathbf{k}$-space. The Dirac point (in which two spin subbands intersect) for $\gamma < 1$ is located at an energy of $\varepsilon_D = 0$ in a point with coordinates $(k_x = 0, k_y = 0)$ of the $\mathbf{k}$-space.

The presence of a parallel magnetic field leads to a greater variety of the Fermi contours and their substantial rearrangement. A typical energy landscape corresponding to the dispersion Equation (2) is shown in **Figure 1**. The magnetic field displaces
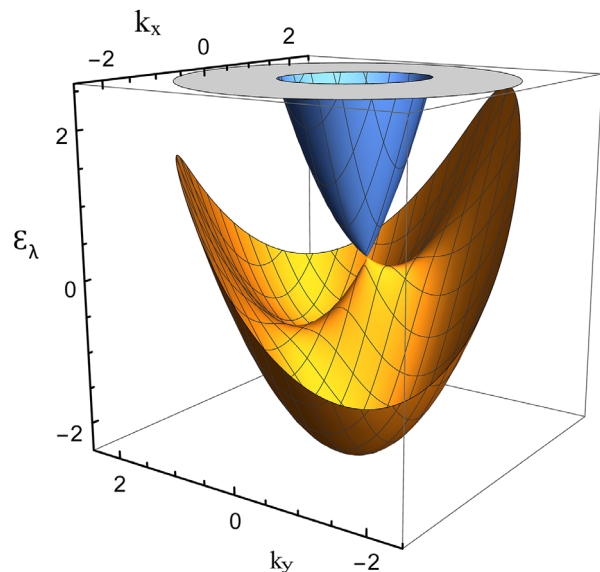

Figure 1. The energy landscape defined by the Equation (2) in $\mathbf{k}$-space. Blue and yellow surfaces correspond to $\lambda = +$ and $\lambda = -$, respectively, and their intersection is a Dirac point. The ratio of the SOI constants $\gamma = 0.3$, the magnetic field strength $b = 0.3$, and direction $\zeta = \pi/2$.

ADVANCED
SCIENCE NEWS
www.advancedsciencenews.com

physica pssb
status solidi
www.pss-b.com

both saddle points and minimums in energy and in the **k**-space. The characteristic dependencies of the energy of critical points (minimums and saddle points) on an orientation of the magnetic field are shown in **Figure 2**. It is seen that when the magnetic field is in the direction of $\zeta = \pi/4$, the difference in the energy minimums is maximal while the energies of the saddle points coincide. At $\zeta = 3\pi/4$, vice versa, the energy minimums coincide and the difference in the saddle point energies is maximal, with the scale of the energy difference increasing with magnetic field.

In addition to numerical calculations of the characteristic energies shown in Figure 2, analytical results for $\zeta = \pi/4$ and $\zeta = 3\pi/4$ are also very useful to find the SOI parameters and g-factor. Expressions for critical points can be easily obtained by transferring the origin of the coordinate axis in **k**-space to a Dirac point and investigating the obtained dispersion law in this space.[23] As a result, we obtain the following expressions for critical points of the spectrum.

For small magnetic fields $b < b_{c1}$ in the direction $\zeta = \pi/4$, we have two energy minimums

$$\varepsilon^m_{-1,2} = -(1 + \gamma)^2 \mp 2b \tag{6}$$

and two saddle points with the same energy

$$\varepsilon^s_{-1,2} = -(1 - \gamma)^2 + b^2/(4\gamma) \tag{7}$$

For $b = b_{c1}$ the minimum ε^m_{-2} transforms to a saddle point, which disappears when $b = b_{c2}$.
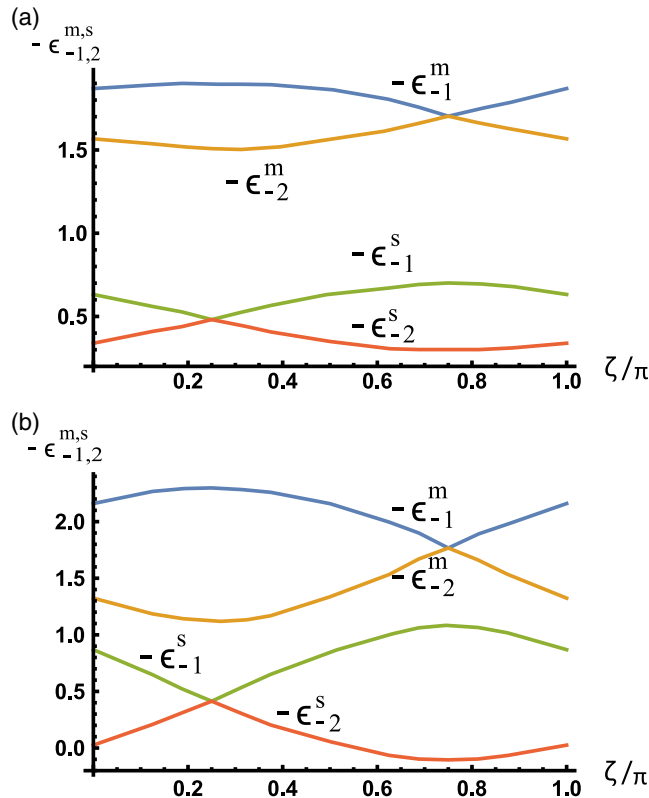

Figure 2. Dependencies of the characteristic energies (minimum $\varepsilon^m_{-1,2}$ and saddle points $\varepsilon^s_{-1,2}$) on the angle of of the magnetic field orientation ζ(rad.): a) for the ratio of the SOI parameters $\gamma = 0.3$ and $b = 0.1$; b) for $\gamma = 0.3$ and $b = 0.3$.

In the case of a small magnetic field $b < b_{c1}$, and $\zeta = 3\pi/4$, the energy landscape in **k**-space has two minimums with equal energies

$$\varepsilon^m_{-3,4} = -(1 + \gamma)^2 - b^2/(4\gamma) \tag{8}$$

and two saddle points spaced in **k**-space

$$\varepsilon^s_{-3,4} = -(1 - \gamma)^2 \mp 2b \tag{9}$$

In a magnetic field $b = b_{c1}$, the minimums $\varepsilon^m_{-3,4}$ and the saddle point ε^s_{-3} turn into one degenerate critical point (minimum), and for the fields $b > b_{c1}$ right down to the fields $b = b_{c2}$ there remain one minimum and one saddle point with energies

$$\varepsilon^{m,s}_{-3} = -(1 \pm \gamma)^2 \mp 2b \tag{10}$$

For both directions $\zeta = \pi/4$ and $\zeta = 3\pi/4$, there are two critical fields at which a substantial rearrangement of the spectrum occurs

$$b_{c1} = 4\gamma \tag{11}$$

and

$$b_{c2} = \begin{cases} (1 + \gamma)^2, & \text{for } \zeta = \pi/4 \\ (1 - \gamma)^2, & \text{for } \zeta = 3\pi/4 \end{cases} \tag{12}$$

In addition, for the angle $\zeta = \pi/4$, the restriction $\gamma \neq 1$ arises due to the requirement $\varepsilon^m_{-1,2} < \varepsilon_d$. Moreover, for $\gamma = 1$, the saddle point is absent. For the angle $\zeta = 3\pi/4$, the region of magnetic fields, where a second singularity ε^s_{-4} appears, is limited by the inequality $b \leq (1 - \gamma)^2$, which arises from the requirement $k_{-s4} \geq 0$. Here k_{-s4} is the module of the vector **k** where the energy ε^s_{-4} is achieved.

Despite the great variety of Fermi contours and their variation depending on the value and direction of the magnetic field, as well as the ratio of the SOI parameters, only the critical points are actually important for a single-particle density of states. The saddle points result in the van Hove singularities and minimums cause the jumps in the density of states. The characteristic densities of states are shown in **Figure 3** for the cases with and without a magnetic field. In panel (c), we present also the dependence of the surface concentration on the position of the Fermi level $Q_S(\varepsilon_F)$ calculated for the same parameters as in panel (b). It is noteworthy that the jump in the density of states causes a noticeable change in the slope of the dependence Q_S versus ε_F, while the sharp peaks in the density of states due to the saddle points are almost invisible.

Therefore, if, as a first approximation, we focus on a change in the density of states, then we can suppose that the transport properties have the peculiarities due to jumps and peaks in the density of states when the Fermi level is in the lower spin subband.[17,18,27,29–32] So we will consider the concentration region when the Fermi level is below the Dirac point, although the 2DEG concentration can be quite large for materials with a large SOI.[27]

In the following section, we show that the critical points in the spectrum lead to peculiarities in the transport properties of the
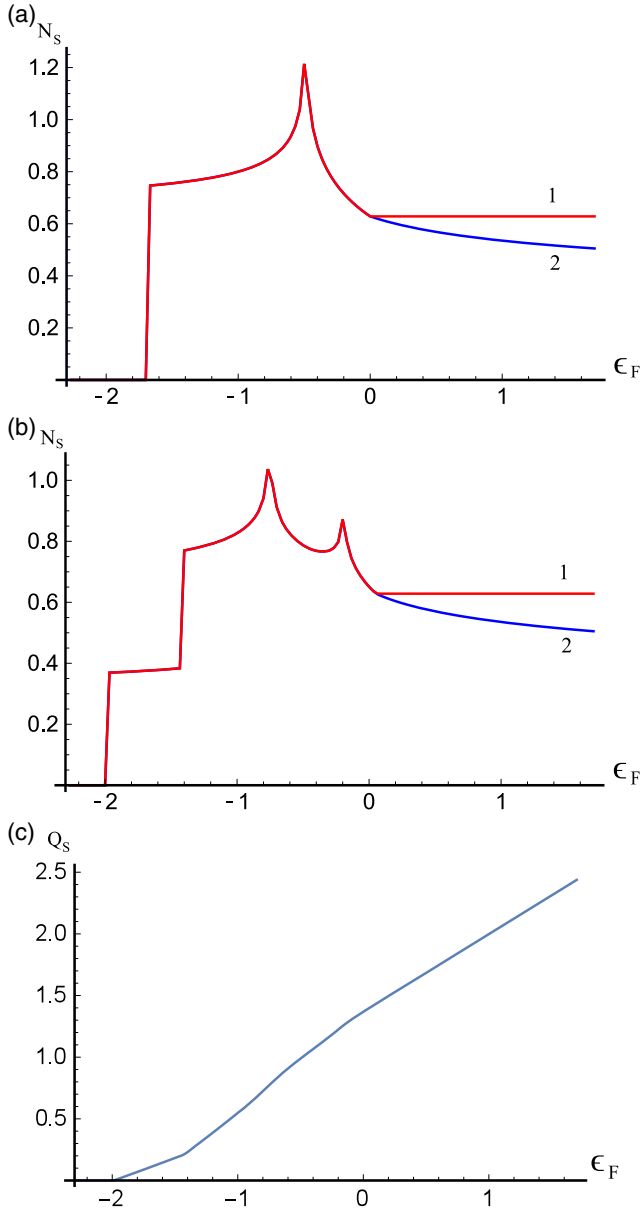
Figure 3. Characteristic densities of states as a function of energy without and with a magnetic field: a) $b = 0$, $\gamma = 0.3$; b) $\gamma = 0.3$, $b = 0.2$, $\zeta = \pi/2$. In both figures, curve 1 shows the total density, and curve 2 is the density of states in the lower spin subband; their intersection means the appearance of a second spin subband (Dirac point). c) The surface charge density as a function of energy for the same parameters as in (b). We note that the energy is normalized to E_{so}, and the normalized density of states above the Dirac point is $N_o = m/(\pi \hbar^2)$.

system when the Fermi level is changed at a given magnetic field or when the magnetic field is changed at a given Fermi level.

3. Boltzmann Kinetic Equation

The electron current is studied using the semiclassical approximation. For a small uniform electric field $\mathscr{E}$, the distribution function $f(\mathbf{k})$ is determined by the Boltzmann equation.[33]

The anisotropy of the energy dispersion leads to the scattering anisotropy, so the collision integral cannot be simplified by introducing a relaxation time. This problem was discussed in detail in the literature.[14–16,34,35]

We consider the scattering by impurities with a short-range potential $V(r) = V_0 \delta(\mathbf{r})$. The concentration of impurities N is assumed to be sufficiently small so that their potentials do not overlap and the scattering by different impurities are not correlated. Using the wave functions (3) and calculating the scattering probability in the Born approximation, we obtain the following equation for the nonequilibrium part of the distribution function $\Delta f_\lambda(\mathbf{k})$

$$\sum_{\lambda'} \int \frac{d^2 k'}{\pi} (1 + \lambda \lambda' \cos[\varphi(\mathbf{k}) - \varphi(\mathbf{k}')]) \delta(\varepsilon_\lambda(\mathbf{k}) \tag{13}$$
$$- \varepsilon_{\lambda'}(\mathbf{k}'))[\Delta f_\lambda(\mathbf{k}) - \Delta f_{\lambda'}(\mathbf{k}')] = \frac{e \mathscr{E} \mathbf{v}_\lambda(\mathbf{k})}{R} \frac{\partial f_0}{\partial \varepsilon}$$

where dimensionless quantities are used. The electric field $\mathscr{E}$ is normalized to $E_{so} k_{so}/e$, group velocity $v_\lambda = \nabla_k \varepsilon_\lambda$, f_0 is the equilibrium distribution function, R is the numerical parameter: $R = V_0^2 N / \alpha^2$.

We rewrite the nonequilibrium part of the distribution function in the following form

$$\Delta f_\lambda(\mathbf{k}) = \frac{e \mathscr{E}}{R} \mathscr{F}_\lambda(\mathbf{k}) \frac{\partial f_0}{\partial \varepsilon} \tag{14}$$

The function $\mathscr{F}_\lambda(\mathbf{k})$ is determined by the equation, which can be easily obtained in the case of zero temperature by integrating with respect to the modulus of $\mathbf{k}$ in Equation (13). In this case, the integration is performed over the Fermi contours. As in some cases the contours have complex shapes, $k(\phi)$ is a multi-valued function of ϕ, so we have to divide the contours into parts for which $k(\phi)$ becomes a single-valued function. Each part is marked by the index r, which can vary from 1 to 4 depending on the shape of the Fermi contour. We will add this index to the notation of the functions defined on the corresponding Fermi contours. It is noteworthy that the similar behavior was considered in the case of SOI only of Rashba type (see ref. [17] for more details).

The function $\mathscr{F}_{\lambda,r}(\mathbf{k})$ on the corresponding part of the Fermi contour $k = k_{\lambda,r}(\phi)$ is defined by the equation

$$\sum_{\lambda',r'} \int \frac{d\phi'}{\pi} (1 + \lambda \lambda' \cos[\varphi_{\lambda,r}(\phi) - \varphi_{\lambda',r'}(\phi')]) \tag{15}$$
$$M_{\lambda',r'}(\phi')[\mathscr{F}_{\lambda,r}(\phi,\theta) - \mathscr{F}_{\lambda',r'}(\phi',\theta)] = \mathscr{G}_{\lambda,r}(\phi,\theta)$$

where

$$M_{\lambda,r}(\phi) = \left[k / \frac{\partial \varepsilon_\lambda(\mathbf{k})}{\partial k} \right]_{k = k_{\lambda,r}(\phi)} \tag{16}$$

$$\varphi_{\lambda,r}(\phi) = \varphi(\mathbf{k})|_{k = k_{\lambda,r}(\phi)} \tag{17}$$

$$\mathscr{G}_{\lambda,r}(\phi,\theta) = \frac{v_\lambda(\mathbf{k}) \cos[\xi(\mathbf{k}) - \theta]}{R} \Big|_{k = k_{\lambda,r}(\phi)} \tag{18}$$

Here $\xi(\mathbf{k})$ is the angle between $\mathbf{v}_{\lambda,r}(\phi)$ and the x axis, θ is the angle between $\mathscr{E}$ and the x axis. The values $M_{\lambda,r}(\phi)$, $\varphi_{\lambda,r}(\phi)$, and

$\mathcal{G}_{\lambda,r}(\phi,\theta)$ are determined on the corresponding Fermi contours. They can be easily calculated using Equation (2).

Equation (15) is a linear Fredmholm equation with a degenerate kernel and it can be solved analytically. Representing its kernel as the sum of the products of the functions of ϕ and ϕ' (these functions are actually sines and cosines), we come to the following form of the function $\mathcal{F}_{\lambda,r}(\phi,\theta)$

$$\mathcal{F}_{\lambda,r}(\phi,\theta)$$
$$= \frac{\mathcal{G}_{\lambda,r}(\phi,\theta) + \mathfrak{A}(\theta) + \lambda\mathfrak{B}(\theta)\cos[\varphi_{\lambda,r}(\phi)] + \lambda\mathfrak{C}(\theta)\sin[\varphi_{\lambda,r}(\phi)]}{A + \lambda B\cos[\varphi_{\lambda,r}(\phi)] + \lambda C\sin[\varphi_{\lambda,r}(\phi)]} \quad (19)$$

The coefficients A, B, C can be directly calculated from Equation (15), as the electron dispersion law is known (2). However, the coefficients $\mathfrak{A}$, $\mathfrak{B}$, and $\mathfrak{C}$ are determined by integrals containing unknown functions $\mathcal{F}_{\lambda,r}(\phi,\theta)$. To obtain a system of equations that will allow us to find the coefficients $\mathfrak{A}$, $\mathfrak{B}$, and $\mathfrak{C}$, we substitute Equation (19) into Equation (15).

As a result, we obtain a system of linear algebraic equations for these coefficients. To find the conductivity it is enough to carry out a calculation for the orientation of the electric field in the x and y directions ($\theta = 0$ and $\theta = \pi/2$). It should be noted that the determinants of the resulting systems are zero, the additional determinants are also zero. This indicates the compatibility of the obtained systems and the lack of equations for determining the desired coefficients ($\mathfrak{A}$, $\mathfrak{B}$, and $\mathfrak{C}$). Therefore, one of the equations in each resulting system is replaced by the equation of electroneutrality

$$\sum_{\lambda,r} \int d\phi M_{\lambda,r}(\phi)\mathcal{F}_{\lambda,r}(\phi,\theta) = 0 \quad (20)$$

Now we are convinced that the determinants of the obtained systems for the orientations of the electric field $\theta = 0$ and $\theta = \pi/2$ are not equal to zero, and can solve the problem. We find the corresponding coefficients $\mathfrak{A}$, $\mathfrak{B}$, and $\mathfrak{C}$, substitute them into Equation (19), and determine the nonequilibrium electron distribution for these orientations of the electric fields in the form (19). A more detailed description of solving the kinetic equation can be found in ref. [17].

4. Conductivity Tensor

Using Equation (19) for the distribution function, we find the dimensionless components of the conductivity tensor normalized to $e^2/(hR)$

$$G_{xx} = \sum_{\lambda,r} \int \frac{d\phi}{2\pi} M_{\lambda,r}(\phi) v_{\lambda,r}(\phi) \cos[\xi_{\lambda,r}(\phi)] \mathcal{F}_{\lambda,r}(\phi,0) \quad (21)$$

$$G_{yy} = \sum_{\lambda,r} \int \frac{d\phi}{2\pi} M_{\lambda,r}(\phi) v_{\lambda,r}(\phi) \sin[\xi_{\lambda,r}(\phi)] \mathcal{F}_{\lambda,r}(\phi,\pi/2) \quad (22)$$

$$G_{xy} = \sum_{\lambda,r} \int \frac{d\phi}{2\pi} M_{\lambda,r}(\phi) v_{\lambda,r}(\phi) \cos[\xi_{\lambda,r}(\phi)] \mathcal{F}_{\lambda,r}(\phi,\pi/2) \quad (23)$$

$$G_{yx} = \sum_{\lambda,r} \int \frac{d\phi}{2\pi} M_{\lambda,r}(\phi) v_{\lambda,r}(\phi) \sin[\xi_{\lambda,r}(\phi)] \mathcal{F}_{\lambda,r}(\phi,0) \quad (24)$$

The results of the conductivity tensor calculations are presented in **Figure 4**. Two measurement modes are described: 1) the Fermi energy is changed at a fixed magnetic field $b = 0$, here ($G_{xx} = G_{yy}$, $G_{xy} = G_{yx}$) see Figure 4a, and 2) the value of the magnetic field along the direction $\zeta = 0$ is changed at a fixed Fermi energy $\varepsilon_F = -0.5$, here ($G_{xy} = G_{yx}$) see Figure 4b. The density of states approximately has the form shown in Figure 3a.

Of greatest interest is a sharp decrease in conductivity near the van Hove singularity, as well as a change in the direction of the maximal conductivity. In the absence of a magnetic field, the diagonal components of the conductivity tensor coincide. In the presence of a magnetic field, the off-diagonal components coincide and their value is an order of magnitude smaller than the diagonal ones. The presence of the off-diagonal components in the zero magnetic field means the appearance of the Hall voltage, with its sign changing near the van Hove singularity. We would also like to note that above the Dirac point the anisotropy practically disappears, which is consistent with the results obtained in the absence of a magnetic field.[15] The minimums in the $\varepsilon(\mathbf{k})$ landscape, leading to jumps in the density of states, cause an increase in the slope of the dependence $G_{xx,yy}(\varepsilon_F)$ and $Q_S(\varepsilon_F)$, which makes it possible to determine these energies.
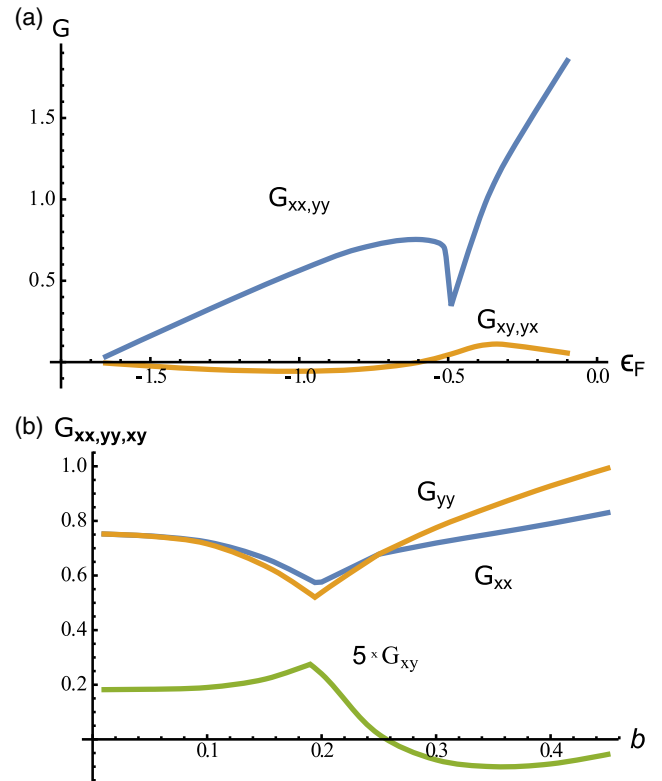

Figure 4. The conductivity tensor components as functions of the Fermi energy and the magnetic field. a) The Fermi energy is changed at $b = 0$. The ratio of the SOI constants is $\gamma = 0.3$. b) The magnetic field is changed at $\varepsilon_F = -0.5$, with $\gamma = 0.3$ and $\zeta = 0$.

5. Determination of the SOI Parameters and the g-Factor

We have shown that the critical points of the spectrum lead to the peculiarities of the conductivity tensor. Therefore, observing these peculiarities in an experiment, we can determine the parameters of the SOIs and g-factor. As an example, let us determine the energies of three saddle points at a fixed magnetic field for two its orientations $\zeta = \pm\pi/4$. These energies $\varepsilon^s_{-1,2,3}$, with a corresponding restriction on the value of the magnetic field, are determined by Equation (9) and (7). Using these relations and going to the dimensional quantities $(E^s_{-1,3,4})$, we easily find

$$\gamma = 1 + \alpha_1 - (2\alpha_1 + \alpha_1^2)^{1/2} \tag{25}$$

$$E_{\text{so}} = -\frac{E^s_{-3} + E^s_{-4}}{2(1 - \gamma)^2} \tag{26}$$

$$b = (E^s_{-4} - E^s_{-3})/(4E_{\text{so}}) \tag{27}$$

where $\alpha_1 = 16(E^s_{-3} + E^s_{-4})(E^s_{-3} + E^s_{-4} - 2E^s_{-1})/(E^s_{-4} - E^s_{-3})^2$.

Another possible option is to find the energy of the saddle points $E^s_{-1,2}$ corresponding to the magnetic field in the direction of $\zeta = +\pi/4$ and determined by Equation (9) and use the energy E^m_{-3} with magnetic field orientation $\zeta = 3\pi/4$, which corresponds to a jump in the density of states and a change in the slope of $G_{xx,yy}(\varepsilon_F)$ or $Q_S(\varepsilon_F)$; see Equation (8). Using these relationships, it is easy to find

$$\gamma = (\alpha_2 - 1)/(\alpha_2 + 1) \tag{28}$$

$$E_{\text{so}} = \frac{E^s_{-2} - E^s_{-1} - 2E^m_{-3}}{2(1 + \gamma)^2} \tag{29}$$

$$b = (E^s_{-2} - E^s_{-1})/(4E_{\text{so}}) \tag{30}$$

where $\alpha_2 = ((2E^m_{-3} + E^s_{-1} - E^s_{-2})/(E^s_{-1} + E^s_{-2}))^{1/2}$.

Here $\gamma = \beta/\alpha$ is the ratio of the Dresselhaus and Rashba SOI constants, $\alpha = (2E_{\text{so}}\hbar^2/m)^{1/2}$ and $g = 2m\alpha^2 b/\mu_B B\hbar^2$.

Note that the assumption of the isotropy of the g-factor is not always satisfied.[36] The proposed method allows us to study the anisotropy of the g-factor. To do this, the following iteration procedure can be used. First, using the proposed methods, we determine E_{so} and γ, then using critical points, we can restore $g_0(\zeta)$. The energy distance between critical points strongly depends on the magnetic field, and for a fixed value of the field, it depends on the g-factor (see Figure 2). Therefore, measuring the distance between saddle points, we find $g_0(\zeta)$ in the zero approximation. Substituting this dependence into the kinetic equation and solving it, we can find $g_1(\zeta)$; repeating this procedure n times, we find $g_n(\zeta)$ in nth approximation with a given accuracy.

In a somewhat simplified form, the system under study is a capacitor with two metal plates (gate and 2DEG), so the charge on it S^*Q_S is equal to CV where C and V are geometric capacitance and voltage between plates, respectively. Its connection with the position of the Fermi level is determined by the relationship

$$Q_S(E_F) = \int_{E_{-m1}}^{E_F} N_S(E)dE \equiv C_1 N_0(E^m_{-2} - E^m_{-1}) + C_2 N_0(E_F - E^m_{-2}) \tag{31}$$

where C_1 and C_2 are constants of the order of $1/2$ and 1 determined from the density graph (see Figure 3b), being weakly dependent on the parameter γ. Recall that as soon as the second spin subband begins to fill, the density of states is $N_o = m/(\pi\hbar^2)$ (see Figure 3b). Moreover, it is seen from Figure 3c that the presence of van Hove singularities practically does not affect this ratio. Thus, by measuring Q_S or V, we can find the critical points $(E^m_{-1,-4})$, and therefore, according to Equation (25)–(30), we can determine the SOI parameters and g-factor.

6. Conclusion

The approach developed previously to study an anisotropic transport in a 2DEG in the framework of the Boltzmann kinetic equation[17] has been used to calculate the conductivity tensor of a 2DEG gas with the Rashba and Dresselhause SOIs in a parallel magnetic field. This method allowed us to find the nonequilibrium distribution function for scattering by impurities with a short-range potential at zero temperature considering electron transitions both within a single Fermi contour and between different contours. An important factor determining the anisotropy of the conductivity is the presence of the van Hove singularity that arises due to the combined effect of the SOI and magnetic field. The energy position of the singularities is controllable by the strength and orientation of the magnetic field in a wide range of the energy.

The conductivity has a sharp dip when the Fermi level passes through the van Hove singularity. This peculiarities of the conductivity have been known for a long time,[37] and to date they attract much interest of researchers.[38] Our results agree qualitatively with the results obtained for other systems.

It has been shown that the minimums in the dispersion law $\varepsilon_\lambda(\mathbf{k})$ cause a significant change in the slope of the dependence of the surface charge Q_S on ε_F, while the van Hove singularities are almost invisible in this dependence. Thus, the measurement of the surface charge and the conductivity tensor can complement each other to find the position of the critical points.

Interesting fact is also a change in the direction of the conductivity anisotropy axis with the Fermi level. The direction of the maximal conductivity rotates when ε_F passes near the van Hove singularity, as in the case when only the Rashba SOI acts.[17] The conductivity anisotropy leads to the appearance of a Hall voltage in a zero magnetic field which changes its sign near the van Hove singularity (see Figure 4a).

Determination of the energy of the conductivity dips or jumps in the density of states at different orientations of the magnetic field allows us to define the Rashba and Dresselhaus SOI constants and the Landé factor. Defining of the parameters of the SOI from changes in the position of the Fermi level or the magnetic field strength also makes it possible to find the dependence of the g-factor on B.

The proposed methods can be easily generalized to the case of a more complex dispersion law, for example, with a SOI term cubic in momentum.

task and partially supported by the Russian Foundation for Basic Research, project No. 20-02-00126.

Conflict of Interest

The author declares no conflict of interest.

Data Availability Statement

Research data are not shared.

Keywords

critical points, in-plane magnetic fields, spin–orbit interactions, two-dimensional electron gas

[1] J. Zutic, J. Fabian, S. Das Sarma, *Rev. Mod. Phys.* **2004**, *76*, 323.
[2] J. Fabian, A. Matos-Abiague, C. Ertler, P. Stano, I. Zutic, *Acta Phys. Slovaca* **2007**, *57*, 565.
[3] Y. A. Bychkov, E. I. Rashba, *JETP Lett.* **1984**, *39*, 78.
[4] G. Dresselhaus, *Phys. Rev.* **1955**, *100*, 580.
[5] L. P. Rokhinson, L. N. Pfeiffer, K. W. West, *Phys. Rev. Lett.* **2006**, *96*, 156602.
[6] C. Yan, S. Kumar, K. Thomas, P. See, I. Farrer, D. Ritchie, J. Grisoths, G. Jones, M. Pepper, *Phys. Rev. Lett.* **2018**, *120*, 137701.
[7] A. Usher, A. Elliott, *J. Phys: Condens. Matter* **2009**, *21*, 103202.
[8] M. A. Wilde, D. Grundler, *New J. Phys.* **2013**, *15*, 115013.
[9] S. D. Ganichev, L. E. Golub, *Phys. Status Solidi B* **2014**, *251*, 1725.
[10] V. M. Pudalov, *arXiv:2008.05451*, **2020**.
[11] A. Sasaki, S. Nonaka, Y. Kunihashi, M. Kohda, T. Bauernfeind, T. Dollinger, K. Richter, J. Nitta, *Nat. Nanotechnol.* **2014**, *9*, 703.
[12] Y. Y. Tkach, *JETP Lett.* **2016**, *104*, 105.
[13] L. van Hove, *Phys. Rev.* **1953**, *89*, 1189.
[14] J. Shliemann, D. Loss, *Phys. Rev. B* **2003**, *68*, 165311.
[15] M. Trushin, J. Shliemann, *Phys. Rev. B* **2007**, *75*, 155323.
[16] K. Vyborny, A. A. Kovalev, J. Sinova, T. Jungwirth, *Phys. Rev. B* **2009**, *79*, 045427.
[17] V. A. Sablikov, Y. Y. Tkach, *Phys. Rev. B* **2019**, *99*, 035436.
[18] V. A. Sablikov, Y. Y. Tkach, *Semiconductors* **2018**, *52*, 1581.
[19] A. Aronov, Y. B. Lyanda-Geller, *JETP Lett.* **1989**, *50*, 431.
[20] V. Edelstein, *Solid State Commun.* **1990**, *70*, 233.
[21] E. L. Ivchenko, S. D. Ganichev, *arXiv:1710.09223*, **2017**.
[22] R. Winkler, *Spin-orbit Coupling Effects in Two-Dimensional Electron and Hole Systems*, Springer Tracts in Modern Physics, Vol. *191*, Springer, Berlin/Heidelberg **2003**.
[23] I. V. Kozlov, Y. A. Kolisnichenko, *Phys. Rev. B* **2019**, *99*, 085129.
[24] S. Maiti, D. L. Maslov, *Phys. Rev. B* **2017**, *95*, 134425.
[25] F. Perez, F. Baboux, C. A. Ullrich, I. D. Amico, G. Vignale, G. Karczewski, T. Wojtowicz, *Phys. Rev. Lett.* **2016**, *117*, 137204.
[26] F.-X. Xiang, X.-L. Wang, M. Veldhorst, S. X. Dou, M. S. Fuhrer, *Phys. Rev. B* **2015**, *92*, 035123.
[27] V. Brosco, L. Benfatto, E. Cappelluti, C. Grimaldi, *Phys. Rev. Lett.* **2016**, *116*, 166602.
[28] E. P. Nakhmedov, O. Alekperov, *Eur. Phys. J. B* **2012**, *85*, 298.
[29] M.-C. Chang, *Phys. Rev. B* **2005**, *71*, 085315.
[30] V. A. Sablikov, Y. Y. Tkach, *Phys. Rev. B* **2007**, *76*, 245321.
[31] Y. Y. Tkach, V. A. Sablikov, A. A. Sukhanov, *J. Phys.: Condens. Matter* **2009**, *21*, 125801.
[32] A. Johansson, J. Henk, I. Mertig, *Phys. Rev. B* **2016**, *93*, 195440.
[33] I. Mertig, *Rep. Prog. Phys.* **1999**, *62*, 237.
[34] P. Schwab, R. Raimondi, *Eur. Phys. J. B* **2002**, *25*, 483.
[35] O. Chalaev, D. Loss, *Phys. Rev. B* **2008**, *77*, 115352.
[36] F. Qu, J. van Veen, F. K. de Vries, A. J. A. Beukman, M. Wimmer, W. Yi, A. A. Kiselev, B.-M. Nguyen, M. Sokolich, M. J. Manfra, F. Nichele, C. M. Marcus, L. P. Kouwenhoven, *Nano Lett.* **2016**, *16*, 7509.
[37] R. Hlubina, *Phys. Rev. B* **1996**, *53*, 11344.
[38] M. E. Barber, A. S. Gibbs, Y. Maeno, A. P. Mackenzie, C. W. Hicks, *Phys. Rev. Lett.* **2018**, *120*, 076602.